Towards a Solid State Far Infrared Laser: Designs, Kinetics and Problems

H N Rutt, Z J Xin, H A Tan

Optoelectronics Research Centre, University of Southampton,
Highfield, Southampton SO17 1BJ, UK.

ABSTRACT

Current far infrared sources of significant average output power are extremely inefficient, bulky gas lasers which are only line tunable, or require liquid helium cooling and high magnetic fields, for example the p-Ge laser. There is increasing interest in this spectral region for possible security, quality control and gas sensing applications. Electrically pumped multiple quantum well structures would be attractive, but suffer from problems of poor mode overlap with the gain region and free carrier loss from mode overlap with carrier injection and extraction regions. We consider the design of an optically pumped multiple quantum well far infrared laser designed to emit in the one hundred micron region. The spectroscopy and kinetics of these structures, measured on the FELIX free electron laser with picosecond time resolution at the pump wavelength near ten microns using pump/probe techniques will be discussed. Strong two photon absorption, leading to long lived free carrier absorption was observed, and represents a potential difficulty for these lasers, although fortunately should be avoidable with suitable designs. Preliminary attempts at laser action are reported.

Keywords: Quantum wells, Far infrared lasers, Lifetime, Pump-probe

1. INTRODUCTION

The spectral region between the carbon dioxide laser lines at 9-11 μm and 1 mm wavelength finds relatively little use in optoelectronics to date. Recently the region has seen increasing interest, and has also been called 'T waves' (terahertz waves) although traditionally it is the far infrared. Sources in the region include optically pumped gas lasers, p-type germanium lasers etc, but all are bulky and often require cryogenic cooling. The 'T wave' source of choice is a picosecond device of very low efficiency, often based on an argon laser pumped titanium sapphire laser which is again expensive, power hungry and bulky. Although potentially compact diode pumped lasers could replace the titanium sapphire system, it remains a very inefficient, intrinsically broad bandwidth source. There is no convenient modest power CW far infrared (FIR) source. There is considerable interest in the possibility of direct electrically pumped quantum cascade lasers in this spectral region. However a major difficulty exists. The long wavelength leads to large modes, with poor overlap with the gain region and extensive overlap with lossy regions containing free carriers.

The traditional FIR gas laser is carbon dioxide laser pumped molecule which achieves inversion between rotational levels of a vibrationally excited state. It is bulky, fragile, requires accurate tuning of the pump laser and limited to those frequencies where a 'good' molecule happens to lase. We can simulate the level scheme of such a laser in a suitably designed quantum well. Initially optical pumping would be with a carbon dioxide laser, but ultimately with a mid infrared quantum cascade laser, to provide a convenient all solid-state source. Free carrier loss can be avoided.

In a symmetric quantum well (QW), electrons can only make photon-induced transitions between subbands with odd quantum number difference. This rule can be broken in an asymmetric QW, for example, a stepped QW which enables a viable optically pumped FIR laser scheme. Asymmetric QWs have found uses in infrared photo-detectors[1] and proposed optically pumped intersubband far-infrared lasers.[2,3] In the latter, the laser relies on the population inversion between the first excited subband and the second subband to which the electrons in the ground subband are optically pumped. The estimated threshold pump power is in the region of 100 kW/cm^2.[2] In this case, the electrons in the excited subbands can be well away from equilibrium lattice temperature and become hot electrons. This can significantly increase non-radiative transitions, particularly by emission of longitudinal optical phonons, and subsequently shorten the lifetime of the electron in the second excited subband. It is thus crucial to know the electron behaviour at high pump intensities. In this paper we report measurements of the kinetics of this system using the FELIX free electron laser by a pump-probe technique.

Correspondence: H. N. Rutt. Email: hnr@ecs.soton.ac.uk.

2. EXPERIMENT

The experiment was conducted using a free electron laser facility (FELIX). A pump-probe technique was applied to measure electron intersubband lifetime. The micro-pulse output of the laser can be of sub-picosecond and peak intensity of tens of MW/cm^2. The setup was detailed in Ref.4. A GaAs/$Al_{1-x}Ga_xAs$ sample was used containing 50 periods of stepped QWs. The nominal parameters and corresponding potential structure are illustrated in Fig. 1.

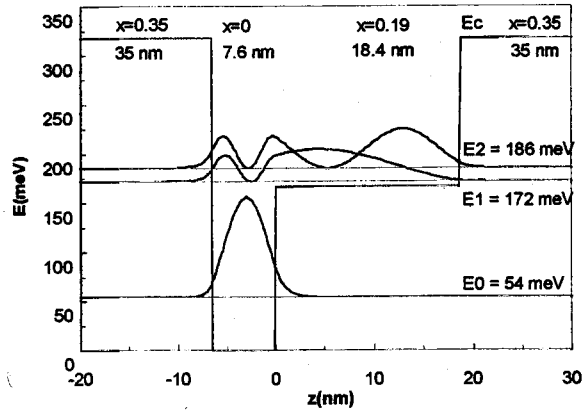

Figure 1. Potential Structure and wavefunctions of a stepped GaAs/AlGaAs QW.

The sample was doped with silicon at a concentration of 2 x 10^{18}/cm^3 and a thickness of 5 nm in the middle of the barriers. The energy difference from the ground level to the second excited level is 132 meV to allow a tunable CO_2 laser pump. The sample was mounted in a liquid helium gas flow cryostat whose temperature is variable from 4K to above room temperature. The sample was firstly measured by a Perkin Elmer FTIR-2000 Fourier transform spectrometer to determine the absorption peak wavelengths. Two peaks were found at λ_1= 9.18 μm and λ_2= 9.95 μm at room temperature and λ_1= 9.19 μm and λ_2= 9.85 μm at 5.6 K as shown in Fig. 2, corresponding to the photon absorptive transitions from E_0 to E_1 and E_2 respectively.

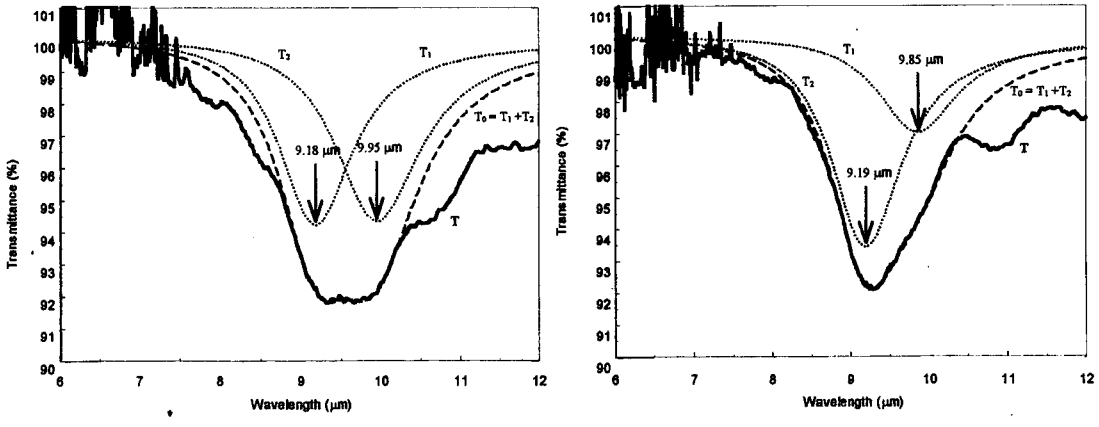

Figure 2. The spectral transmittance of the sample at room temperature (left) and 5.7 K (right) with the source TM polarized and incident at the Brewster angle.

3. RESULTS AND DISCUSSION

Fig. 3 shows the differentially transmission signal of the probe pulse as a function of the delay time relative to the pump pulse at a wavelength 9.35 μm and temperature 4.2 K obtained from the pump-probe experiment. This wavelength is slightly longer than the resonant wavelength between the ground and the second excited subbands, but it is at the peak

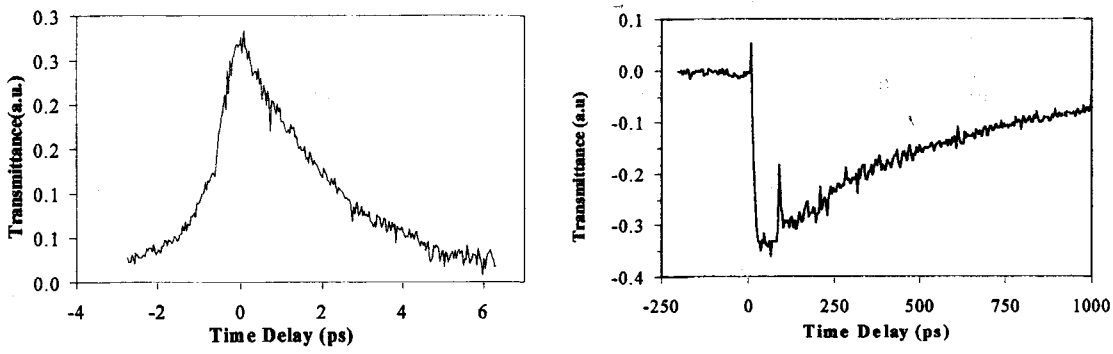

Figure 3. Intersubband lifetime (left), and slow, long lifetime (right).

absorption of the sample as can been in Fig. 2. A 10 dB attenuator was used at the beam output in the measurement. The decay signal corresponds to a 2.5 ps lifetime (left in Fig. 3). This value is several times longer than that obtained from rectangular QWs.[5-6] This can be attributed to the fact that the overlap of the wavefunctions in a stepped QW for the intersubband transition is smaller compared with that in rectangular QWs. More interestingly, when we extended the time scan range to nanoseconds, we found a strong absorptive signal which immediately followed the short positive decay but faded much slowly as shown on the right in Fig. 3. This slow decay has an astonishingly long lifetime of 500 ps. This is compared with normal electron intersubband lifetime of a few picoseconds at most. Fig. 4 shows more data of the slow decay from different experiments as a function of pump power, wavelength and temperature respectively. For clarity, the curves have been shifted vertically from their zero level. We notice in the figure that the slow decay feature disappears at 10 dB attenuation and 12.55 μm pump wavelength, although the peaks at the zero time delay is still visible for those measurements. The absolute power intensity incident on the sample in Fig. 3 was much higher than those in Fig. 4 as a result of more careful optical alignment and focusing.

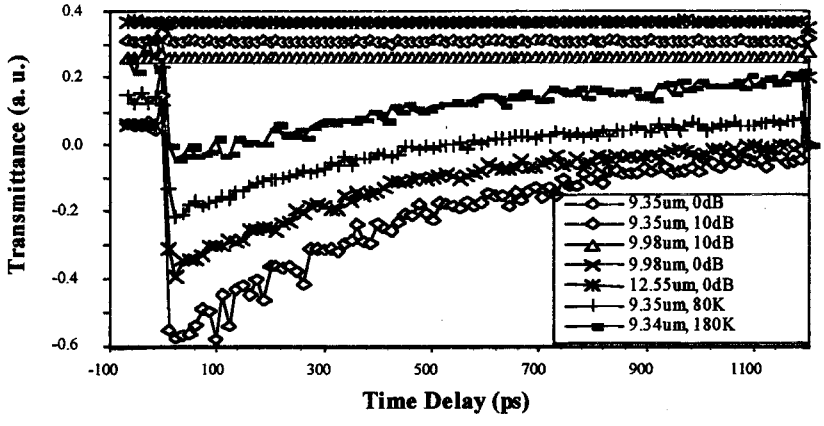

Figure 4. The variation of slow decay with respect to attenuation and temperature.

The strong intensity dependence and disappearance at longer wavelengths of the slow decay suggest that a two-photon process is involved in the pump-probe experiment. At very high power intensities, the first transition subband of the sample can be populated to saturation when the positive differentially transmissive peak appears. Following that, a considerable number of electrons in this excited subband are further pumped to the continuum or quasi-continuum conduction band where they become free electrons and are able to perform 3-D absorption. This is much stronger than the absorption taking place in 2-D environment as the selection rules have been relaxed, so it can overwhelm the absorption decrease caused by the ground subband electron depopulation. The second order nonlinear effect[7] cannot be excluded, due to the asymmetric quantum well structure with very high pump power intensity. In particular this nonlinear effect can be enhanced due to the fact that the energy difference of the ground subband to the bottom of the continuum conduction band in the barrier layers is 264 meV which is coincident with the resonant energy of the second harmonic generation.[8]

To confirm two-photons absorption, a second sample was used with a similar structure of the sample outlined in Fig. 1, but it had a higher barrier potential (x = 0.45). In the case, the potential difference between the ground subband and barrier is greater than two-photon energy, the two-photon effect is minimized. Indeed, from the second sample, in most cases the slow negative decay was unobservable. Weak residual signals in a few cases at very high pump power density probably arise from three photon processes. The very long recombination times suggests that the electrons are removed from the immediate vicinity of the well (where rapid recapture would be expected) into the barrier regions.

4. MODELLING

In order to investigate the feasibility of the two-photon mechanism, we established a three-level model to simulate the process, i.e. the ground subband, excited subband and continuum conduction band as can be seen in Fig. 1. In the model E_0 denotes the ground subband; E_i the excited subbands, which could be the first or second excited subbands in our quantum well structure; the continuum band is represented as E_c, the third level in this model.
The 3-level system model comprises the rate equations and an equation for total population, shown here as Equations 1-3. In these equations, N_0, N_i and N_c represent the electron populations in the ground and excited levels as well as continuum conduction band respectively. The total electron population is N. We have assumed that before the pump pulse is applied, all the electrons are in the ground level, i.e. $N_0 = N$. This assumption is well justified at temperature of 4 K.

$$\frac{dN_0(t)}{dt} = -\frac{\sigma_0}{\hbar\omega} I(t) N_0(t) + \frac{N_i(t)}{\tau_{i0}} + \frac{\sigma_0}{\hbar\omega} I(t) N_i(t) + \frac{N_c(t)}{\tau_{c0}} \tag{1}$$

$$\frac{dN_i(t)}{dt} = \frac{\sigma_0}{\hbar\omega} I(t) N_0(t) - \frac{N_i(t)}{\tau_{i0}} - \frac{\sigma_0}{\hbar\omega} I(t) N_i(t) - \frac{\sigma_i}{\hbar\omega} I(t) N_i(t) + \frac{N_c(t)}{\tau_{ci}} \tag{2}$$

$$N_0(t) + N_i(t) + N_c(t) = N \tag{3}$$

The electron lifetime between energy levels is given as τ_{xy}, where subscript index x and y refer to the energy levels they represent respectively. σ_0 and σ_i are the absorption cross-sections from E_0 to E_i and E_i to E_c respectively. ω is the circular frequency of the pump pulse. The pump pulse $I(t)$ with respect of time t can be best described using a sech function with a peak intensity of I_0 and full width at half maximum (FWHM) of τ_ω, $I(t) = I_0 \operatorname{sec} h(t/0.38\tau_\omega)$. We have used a value of 0.5 ps for τ_ω in our model. The last term in the right hand side of Equation 2, the electron recombination rate from E_c to E_i, is negligible in this experiment as τ_{ci} is much longer than τ_{i0}.

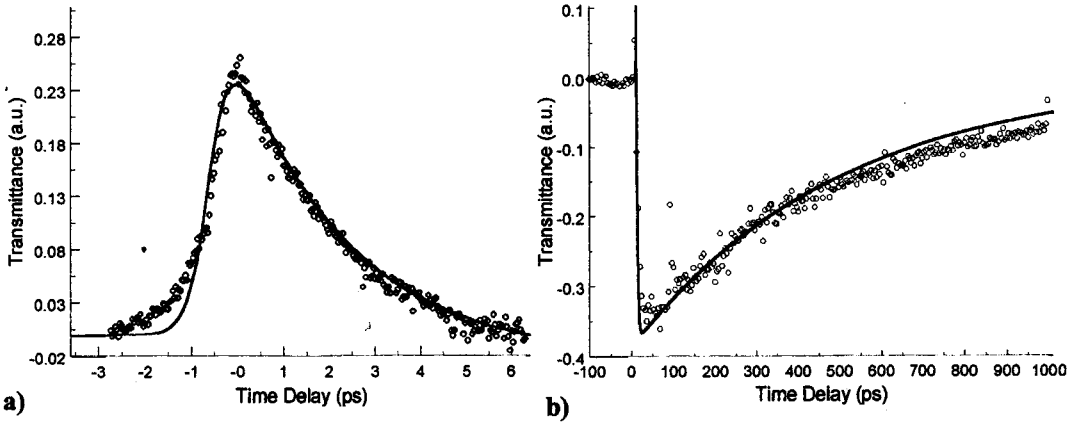

Figure 5. a) The pump-probe intersubband lifetime measurement with the solid line fitted using the rate equation model with intersubband lifetime of 2.5 ps and **b)** the slow decay fitted with a lifetime of 500 ps.

$$S(t_d) = \int_{-\infty}^{+\infty} K \cdot I(t-t_d) \cdot \exp\left[-\sigma_0(N_0 - N_i) + \sigma_i(N_i - N_c) + \sigma_c(N_c)\right] dt_d \quad (4)$$

Equation 4 models the transmission of the probe signal as a function of time delay between the pump and the probe signal where K is an arbitrary constant. The pump and probe pulses in our pump-probe experiment are of the same origin albeit different intensity. Hence, the probe pulse, represented as $I(t-t_d)$ after a time delay t_d with respect to t of the pump pulse, will have the same wavelength, pulse duration, and pulse shape as the pump pulse. The absorption cross section in the continuum conduction band is denoted as σ_c.

Table 1: Parameters used in the rate equation model.

Parameters	Symbols	Values
Total population	N	2×10^{12}
Cross section in E_0 to E_i absorption	σ_0	2.6×10^{-15} cm
Cross section in E_i to E_c absorption	σ_1	$0.8 \times 2.6 \times 10^{-15}$ cm
Cross section in E_c absorption	σ_c	$150 \times 2.6 \times 10^{-15}$ cm
Intersubband electron lifetime	τ_{i0}	2.5 ps
Continuum band to ground subband lifetime	τ_{c0}	500 ps
Pump wavelength	λ_ω	9.35 μm
Pump pulse width	τ_ω	0.5 ps

With the parameters listed in Table 1, we have fitted the experimental result in Fig. 3 using Equation 5. As can be seen in Fig. 5, the fitted result agrees well with the experimental data. The peak pump pulse intensity for the long dacay fit is a factor of ten greater than the one used for the intersubband lifetime fit. It is noticeable that in all cases the strong, long lifetime negative signal is always preceded by a short lifetime, positive saturation signal. The model also reproduces all the features observed in Fig. 4, where scalling the pump intensity reduces the magnitude of the long decay signal, as shown in Fig. 6. The direction of the arrow in the figure indicates increasing pump intensities.

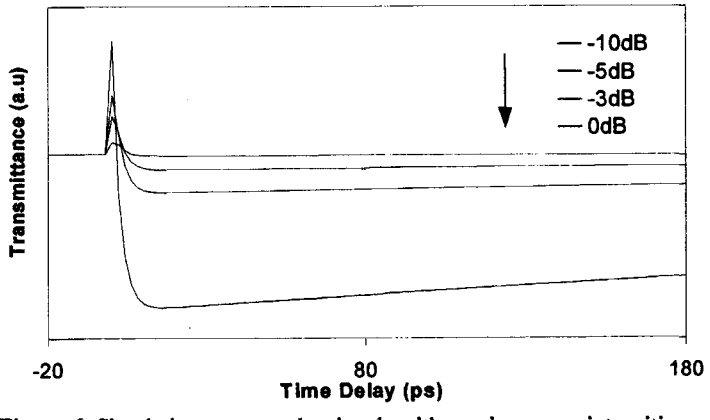

Figure 6. Simulating pump-probe signals with varying pump intensities

5. CONCLUSION

Pump-probe lifetime measurements have been made on a GaAs/AlGaAs sample containing 50 stepped quantum wells. The results show that electrons in the sample have a longer intersubband lifetime than normal rectangular QW. On saturation pumping, multi-photon absorption can be induced. It becomes significant when the multi-photon absorption energy coincides with the resonant energy of the ground subband to the barrier. The free electrons induced by multi-photon absorption result in very strong absorption of the pump light, and would cause severe extra loss to the QW laser emission. Preliminary attempts at pulsed laser action have not so far been successful. However we believe that with redesigned samples based on the FELIX kinetics measurements, which eliminate the parasitic effects of two photon absorption, there are good prospects for a convenient, compact FIR laser based on this technique.

ACKNOWLEDGEMENTS

The authors are sincerely grateful to the EPSRC for funding the research and to the EPSRC Central Facility for III-V Semiconductors at the University of Sheffield for providing the samples. Dr J P Wells and I Bradley provided invaluable assistance with the free electron laser measurements.

REFERENCES

1. B. F. Levine, J. Appl. Phys., **74**(1993), R1
2. Z. Xin and H. N. Rutt, Semicond. Sci. Technol., **12**(1997), 1129
3. S. Borenstain and J. Katz, Appl. Phys. Lett., **55**(1989), 654
4. P. C. Findlay, C. R. Pidgeon, R. Kotitschke, A. Hollingworth, B. N. Murdin, C. J. G. M. Langerak, A. F. G. van der Meer, C. M. Ciesla, J. Oswald, A. Homer, G. Spingholz and G. Bauer, Phys. Rev. B, **58**(1998), 12908.
5. J. Faist, F. Capasso, C. Sirtori, D. L. Sivco, A. L. Hutchinson, S. N G. Chu and A. Y. Cho, Appl. Phys. Lett. **63**(1993), 1354.
6. K. L. Schumacher, D. Collings, R. T. Phillips, D. A. Ritchie, G. Weber, J. N. Schulman and K. Ploog, Semicond. Sci. Technol., **11**(1996), 1173.
7. J. B. Khurgin, Semiconductors and Semimetals, Vol **59**, Ed E. Garmire and A Kost, Academic Press, 1999, Chapter One.
8. After the paper was submitted, further experiment had excluded the possibility of the second harmonic generation being involved. However, the explanation to the slow decay can be given by the deformation of the conduction band around the doping layers caused by the Coulomb potential.